Clim Dyn
DOI 10.1007/s00382-015-2540-2

Global and European climate impacts of a slowdown of the AMOC in a high resolution GCM

L. C. Jackson · R. Kahana · T. Graham · M. A. Ringer · T. Woollings · J. V. Mecking · R. A. Wood

Received: 11 November 2014 / Accepted: 23 February 2015

Abstract The impacts of a hypothetical slowdown in the Atlantic Meridional Overturning Circulation (AMOC) are assessed in a state-of-the-art global climate model (HadGEM3), with particular emphasis on Europe. This is the highest resolution coupled global climate model to be used to study the impacts of an AMOC slowdown so far. Many results found are consistent with previous studies and can be considered robust impacts from a large reduction or collapse of the AMOC. These include: widespread cooling throughout the North Atlantic and northern hemisphere in general; less precipitation in the northern hemisphere midlatitudes; large changes in precipitation in the tropics and a strengthening of the North Atlantic storm track. The focus on Europe, aided by the increase in resolution, has revealed previously undiscussed impacts, particularly those associated with changing atmospheric circulation patterns. Summer precipitation decreases (increases) in northern (southern) Europe and is associated with a negative summer North Atlantic Oscillation signal. Winter precipitation is also affected by the changing atmospheric circulation, with localised increases in precipitation associated with more winter storms and a strengthened winter storm track. Stronger westerly winds in winter increase the warming maritime effect while weaker westerlies in summer decrease the cooling maritime effect. In the absence of these circulation changes the cooling over Europe's landmass would be even larger in both seasons. The general cooling and atmospheric circulation changes result in weaker peak river flows and vegetation productivity, which may raise issues of water availability and crop production.

Keywords Climate · Impacts · AMOC

1 Introduction

The Atlantic Meridional Overturning Circulation (AMOC) plays a very important role in the climate system by transporting heat northwards in the Atlantic [$\sim$1 PW at 30°N, Bryden and Imawaki (2001)]. This circulation is predicted to weaken as the climate warms and the surface waters of the North Atlantic become less dense, inhibiting wintertime convection. There is uncertainty as to the extent of this weakening since the predictions from global climate models (GCMs) vary substantially (Collins et al. 2013) and the AMOC is known to be sensitive to additional fresh water input not fully represented in these GCMs (such as melting from the Greenland ice sheet). Although experiments with estimates of likely additional fresh water input in GCMs have shown only moderate additional weakening (Swingedouw et al. 2013), and none of these have shown a rapid shutdown of the AMOC, studies of paleoclimate data proxies have suggested that large and rapid reorganisations of the ocean currents may have occured in the past (Rahmstorf 2002; Clement and Peterson 2008). There have been suggestions that many GCMs have a bias which might make the AMOC more stable and less sensitive to fresh water inputs (de Vries and Weber 2005; Jackson 2013), although this bias has been removed in some of the current GCMs (Weaver et al. 2012).

L. C. Jackson (✉) · R. Kahana · T. Graham · M. A. Ringer · R. A. Wood
Met Office Hadley Centre, Exeter, UK
e-mail: laura.jackson@metoffice.gov.uk

T. Woollings
University of Reading, Reading, UK

J. V. Mecking
University of Southampton, Southampton, UK

Published online: 11 March 2015

Although a rapid collapse of the AMOC has been assessed to be very unlikely within the twenty first century (Collins et al. 2013), such a collapse would cause large and rapid changes in the climate. Hence it is regarded as a 'low probability-high impact' event, making it important to assess the risk of those impacts. In addition, the magnitude of AMOC decrease in projections of twenty first century greenhouse gas-induced climate change are very varied, with GCMs in the most extreme climate change scenario of the fifth IPCC report suggesting a weakening of 12–54 % by 2100 (Collins et al. 2013). Both Good et al. (2015) and Drijfhout et al. (2012) have shown that temperature changes over Europe when greenhouse gases are increased are dependent on the magnitude of AMOC reduction, and Woollings et al. (2012a, b) have shown that the same is true for changes in the Atlantic storm track and reduction in polar lows. Hence a greater understanding of impacts associated with a decrease in the AMOC will improve our understanding of uncertainties around impacts of anthropogenically forced climate change.

Previous studies have examined the impacts of a decrease in the AMOC through the addition of fresh water into the North Atlantic. These studies have included realistic values or more idealised fresh water forcing set-ups, and have been applied in preindustrial (Vellinga and Wood 2002; Stouffer et al. 2006), future (including increasing greenhouse gases, Vellinga and Wood (2008); Kuhlbrodt et al. (2009)) and paleoclimate conditions (Manabe and Stouffer 1997; Kageyama et al. 2012). Although most studies have concentrated on large scale temperature and precipitation changes, some have investigated the influence on sea level (Levermann et al. 2005), ecosystems and agriculture (Kuhlbrodt et al. 2009) and regional climate changes (Jacob et al. 2005; Chang et al. 2008; Parsons et al. 2014). This study is unique in that it uses the highest resolution coupled global model for such a study. This increased resolution is important for a number of reasons. Firstly, the response of the ocean circulation may be affected by increases in the ocean resolution which permit eddies. Secondly, there are suggestions that increased resolution can improve the atmospheric transport of moisture (Demory et al. 2013) and synoptic variability over Europe (Scaife et al. 2011, 2014). Thirdly, the increased resolution allows a much better representation of orography and local weather patterns. In particular this can improve our assessment of localised impacts.

The model and methods used in this study are presented in Sect. 2. Global impacts are discussed in Sect. 3 and those over Europe in Sect. 4. Section 5 presents the conclusions.

2 Model and methods

2.1 HadGEM3 GC2

The GC2 (Williams et al. 2015) configuration of the HadGEM3 model (Hewitt et al. 2011) is used, consisting of atmosphere, ocean, sea-ice and land-surface models. Fluxes of heat, freshwater and momentum are passed between the atmosphere and ocean-ice components every 3 h while fluxes are passed between the ocean and ice models every ocean model time step (22.5 min).

The atmosphere model is version Global Atmosphere vn6.0 of the Met Office unified model with a horizontal resolution of N216 (approximately 60 km in mid-latitudes). Demory et al. (2013) showed that increased horizontal resolution up to approximately 60 km resulted in an increase in the large-scale water transport from the ocean to the land and that models with resolution of 60 km and finer agreed well with reanalyses. This was interpreted as showing that large-scale storms penetrate further over land in higher-resolution models while at lower resolution there is much more local recycling of water (i.e. it tends to be evaporated and precipitated locally rather than being advected horizontally). Compared to previous generations of climate models, GC2 is notable for a very realistic representation of jet stream variability and does not suffer from an underestimation of midlatitude cyclone intensity (Williams et al. in prep). Scaife et al. (2014) have shown that the seasonal forecast system GloSea5, which is based on HadGEM3 at N216 resolution, can successfully predict the winter North Atlantic Oscillation (NAO) and aspects of European winter variability, although the magnitude of the variability is underestimated. The skill of GloSea5 may be due to the increased resolution since the previous version of the forecast system (at lower resolution) showed low skill outside the tropics (Arribas et al. 2010). There are 85 levels in the vertical meaning that compared to earlier Met Office climate models, GC2 has improved resolution of the stratosphere which is thought to be important for resolving teleconnections including to the Eurasian atmospheric circulation (Ineson and Scaife 2009).

The ocean model is the Global Ocean 5 (GO5; Megann et al. 2013) version of the ORCA025 configuration of the NEMO model (Madec 2008) with a nominal horizontal resolution of 25°. In the southern hemisphere the grid is an isotropic mercator grid: the meridional grid spacing decreases at high latitudes such that the grid cells remain approximately square at high latitude. In the northern hemisphere the grid is a quasi-isotropic bipolar grid with poles over land. The eddy permitting horizontal resolution has been shown to reduce a cold bias off the coast of Grand Banks as a result of an improved Gulf Stream and North Atlantic Drift path in comparison to lower resolution models. The reduction of the cold bias has led to an

improved simulation of Atlantic and European winter blocking (Scaife et al. 2011). Because of the increased horizontal resolution the model no longer uses the GM (Gent and Mcwilliams 1990) parameterisation for horizontal eddy mixing of tracers.

The ocean model has 75 model levels with a thickness of 1m at the surface increasing to approximately 200 m at a depth of 6000 m. The increased vertical resolution in the upper ocean compared to previous Hadley Centre climate models, along with the increased coupling frequency, leads to improved simulation of the diurnal cycle (Bernie et al. 2008). Near surface vertical mixing is carried out using a modified version of the turbulent kinetic energy scheme (TKE; Gaspar et al. 1990; Madec 2008). Unresolved vertical mixing processes are represented by a constant background vertical diffusivity of $1.2 \times 10^{-5}\,\mathrm{m^2\,s^{-1}}$.

The sea ice model is version 4.1 of the Los Alamos National Laboratory sea ice model (CICE Hunke and Lipscomb 2010) and has the same resolution as the ocean model. The model uses elastic–viscous–plastic ice dynamics (Bitz and Lipscomb 1999), energy conserving thermodynamics and five sea ice thickness categories.

The land model used in GC2 is the GL6 configuration of the Joint UK Land Environment Simulator (JULES). The model simulates the state of the soil and 5 vegetation types (broadleaf trees, needleleaf trees, C3 (temperate) grass, C4 (tropical) grass, and shrubs) in each land grid box. The distribution of these plant types is fixed throughout the simulation and represent the world vegetation circa 1980. For this reason the changes from one type of plant to another, that would naturally occur under changing climate are not presented here. We will analyse the vegetation Net Primary Productivity (NPP) as a measure of plant productivity. NPP is calculated in the model as the difference between the gross primary productivity and respiration rate and its changes do not affect the atmospheric CO_2 or other carbon stores since the model does not include a carbon cycle.

The model provides estimates of runoff and river flows for each grid cell, which are then routed across the domain to the river outflow points. The river's network output is at 1 degree resolution which is lower than the atmospheric resolution and therefore only enables us to analyse Europe's biggest rivers. The simulations provide an estimation of the natural flow and do not include the effects of dams, irrigation or other extractions. This should be taken into consideration when comparing with observational data.

2.2 Experimental design

To examine the impact of a shutdown or large reduction of the AMOC we compare a simulation where the salinity is perturbed to cause a reduction of AMOC strength with a long control run. The model was initialised from a development version of GC2 (with only minor model differences) that had been initialised from climatology and spun up for over 36 years. The control run of GC2 has been run for a further 150 years from this time. Since the spin up time was short there is a drift in temperatures and salinities in the control experiment. Drifts in upper ocean temperatures and salinities (calculated as area means in separate basins) range up 0.8 °C/century and 0.1 PSU/century which are smaller than the changes experienced in the experiment where the salinity is perturbed (and much smaller in the case of salinity). To take into account this drift, anomalies are calculated with reference to the same period in the control experiment.

To reduce the length of simulation required we adopt the method of Vellinga and Wood (2002) to induce a collapse of the AMOC. This methodology involves perturbing the salinity in the upper layers of the North Atlantic to inhibit deep convection and hence quickly shut down the AMOC. Vellinga and Wood (2002) found that this method had a similar impact to the more traditional 'hosing' experiments where additional freshwater fluxes are applied to reduce salinity. Although this method of collapsing the AMOC is unrealistic, it is adequate for the purposes of investigating the impacts of a shutdown, but not for giving a credible assessment of the rate of change.

The perturbed experiment is initialised after 42 years of the control run. Instantaneous salinity perturbations are applied to the upper 536 m of the Atlantic and Arctic Ocean north of 20°N each December for the first 10 years of the perturbation run (see Fig. 1). Each salinity perturbation is equivalent to continuously adding freshwater at a rate of 10 Sv ($1\ \mathrm{Sv} = 10^6\,\mathrm{m^3\,s^{-1}}$) for 10 years (total of 100 SvYr). Tapering is applied to the perturbation over 350–536 m to reduce numerical problems that could be caused by unrealistically large density gradients. Similarly, the perturbation was spread over ten years to reduce the model shock associated with the perturbation. As is common practice in hosing experiments the salinity in the rest of the ocean is also perturbed such that the total freshwater content of the global ocean remains constant.

In all of the runs the atmospheric CO_2 concentration is kept constant (at 1980's levels). This means that changes to the vegetation productivity are caused only by the climatic effects of the AMOC decrease (i.e. changes in temperature, and the hydrological cycle) and not by the more direct effect that changes in CO_2 levels have on plant photosynthesis and transpiration (Wiltshire et al. 2013; Hemming et al. 2013). This is an important difference between this experiment and future projections of plant productivity from increasing greenhouse gases, in which plants are affected by both the changing climate and by the physiological CO_2 effects.

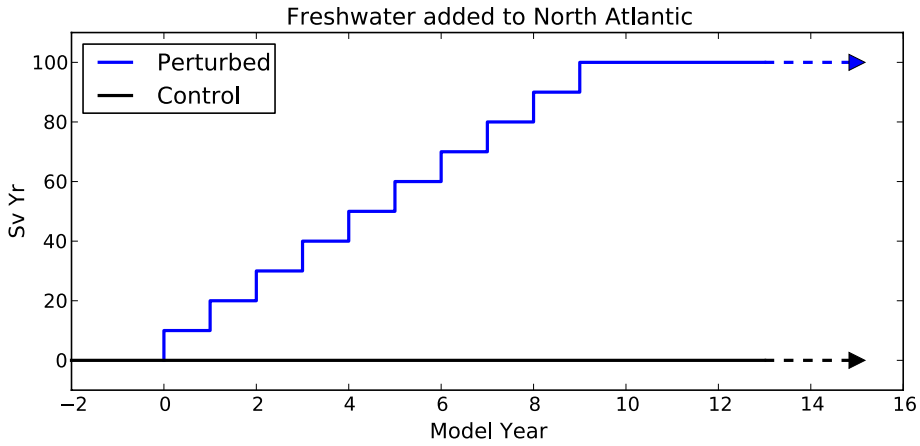

Fig. 1 Cumulative volume of freshwater added to the North Atlantic Ocean (Sv Yr). 10 Sv Yr are added each year for the first 10 years. No further freshwater is added after this time

All averages presented (unless otherwise stated) are for years 60–90 after the start of the freshwater perturbations (50–80 years after the perturbations have ended). Anomalies are presented relative to a 30 year average of the control at the same period. Significance is tested by taking 30 year means of the control simulation with start dates every 10 years and calculating the standard deviation of these mean values. Anomalies are considered significant if they are greater than 2 standard deviations.

3 Global response to an AMOC weakening

The large freshening of the subpolar North Atlantic causes a cessation of convection over the deep water formation regions and a rapid decrease in the strength of the overturning circulation (see Fig. 2). At the end of the freshwater perturbations (year 10), the AMOC strength at 26°N (blue line) partly recovers from a complete shutdown to a level of ~2 Sv. The AMOC decrease and recovery is more gradual in the southern hemisphere (30°S, red line). The AMOC recovery is different from that in the similar experiment of Vellinga et al. (2002) and Vellinga and Wood (2002) where the AMOC strength recovered steadily over ~120 years back to its control strength. In this study the AMOC shows no signs of recovery over the first 100 years of the experiment. This difference may be caused by the greater perturbation of the salinity field (equivalent to 100 SvYr rather than 16 SvYr), or may be a result of different dynamical behaviour in this model, and will be investigated in a future study.

Although there is still a weak overturning cell in the Atlantic, there has been a dramatic decrease in winter mixed later depth in the subpolar gyre. The maximum winter mixed layer depth after the Atlantic freshening is less than 250 m (not shown) suggesting that there is no longer any deep convection. The northwards transport of heat in the Atlantic ocean (measured at 30°N) is more than halved from 1.0 to 0.4 PW (Fig. 2 bottom middle). There is also a reversal in the south Atlantic, with the ocean transporting heat southwards rather than northwards when the AMOC is reduced. As a result, there is widespread surface cooling of the ocean throughout the North Atlantic, cooling of the atmosphere over the North Atlantic and throughout the northern hemisphere (Fig. 2 bottom right and Fig. 3 top) and the northern hemisphere sea ice extends further south in all seasons, even reaching as far south as the northern tip of the UK and the Grand Banks at its greatest extent in March. The cooling is stronger in winter, particularly in the Arctic where the increased ice insulates the atmosphere from the warmer ocean. Cooling is particularly intense in the Barents, Greenland–Iceland–Norway (GIN) and Labrador seas which have experienced the greatest increase in sea ice, with widespread coverage even in summer when the AMOC is reduced. Temperatures in those regions are reduced by up to 15 °C, although the temperature decreases over the Atlantic are more typically 2–5 °C in the subtropical gyre and 5–10 °C in the subpolar gyre. Here we find that the southwards shift of the ITCZ in the Atlantic extends to the other ocean basins causing a global shift to the south in the ITCZ.

Previous studies have reported similar decreases in surface air temperature caused by a reduction of the AMOC, though the amount and extent of cooling, and the reduction of the AMOC vary with model and forcing scenario (Stouffer et al. 2006; Kageyama et al. 2012; Vellinga and Wood 2002). All show the largest cooling over the North Atlantic subpolar gyre, Labrador, GIN and Barents sea regions with some experiments in Stouffer et al. (2006) showing temperature increases north of the hosing regions as a result of northwards shifts in convection. There is a wide range in the zonal extent of the cooling in the northern hemisphere in these studies, with most finding cooling over Europe, some with cooling over parts of Asia and very few with cooling over North America. The results in this study show a greater zonal extent than most, if not all, previous

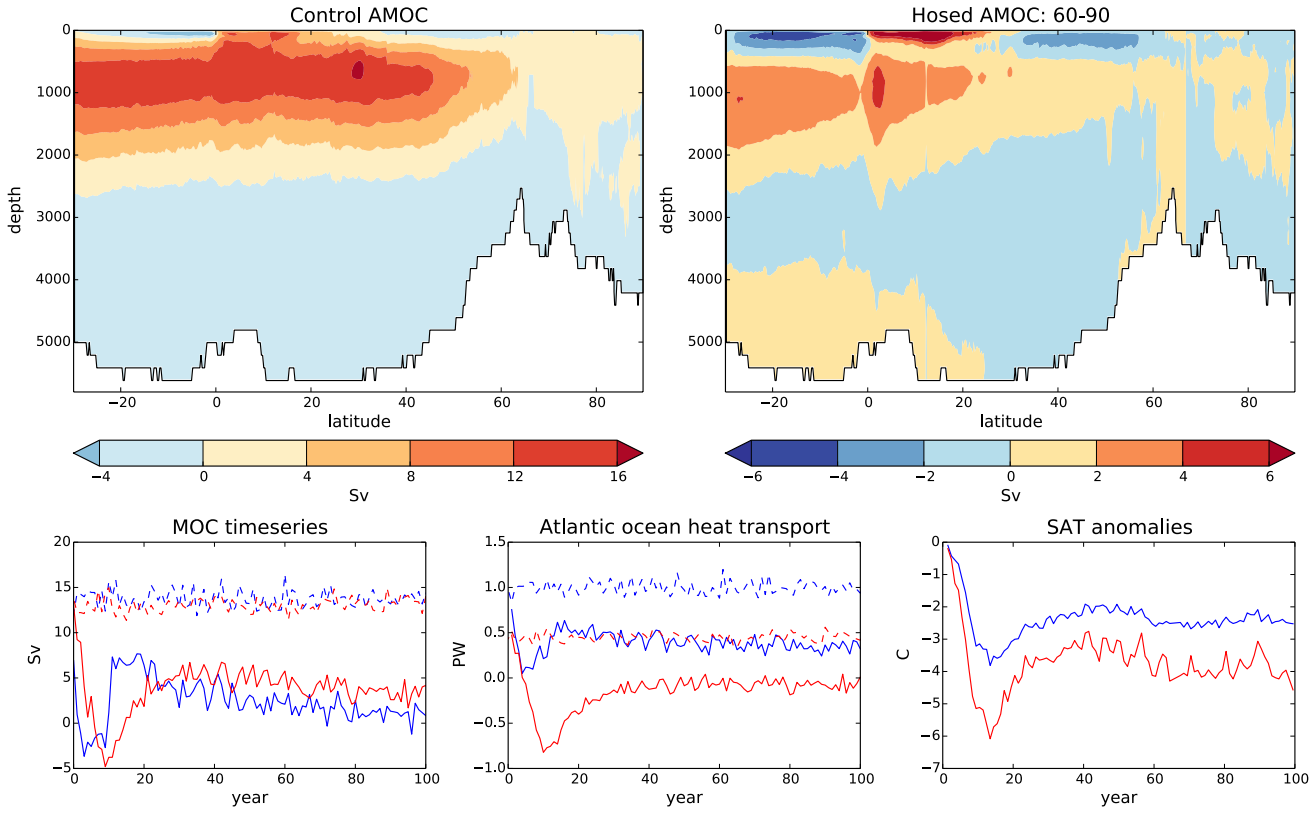

Fig. 2 The Atlantic Meridional Overturning Circulation (AMOC). *Top left* AMOC streamfunctions (Sv) for the control (average of years 60–90). *Top left* AMOC streamfunction (Sv) in the perturbed experiment (average of years 60–90). Note the different scales. *Bottom left* timeseries of AMOC strength at 26°N, 1000 m depth (*blue*) and at 30°S, 1000 m depth (*red*) for the control (*dashed*) and perturbed experiment (*solid*). *Bottom middle* Meridional ocean heat transport at 30°N (*blue*) and 30°S (*red*) in the Atlantic for the control (*dashed*) and perturbed experiment (*solid*). *Bottom right* Anomalies of area averaged SAT for the whole of the northern hemisphere (*blue*) and over the Atlantic (60–0°W, 20–60°N, *red*)

experiments. In common with other studies there is a slight warming across the southern hemisphere, particularly in the south east Atlantic.

Precipitation patterns indicate a southwards shift of the Intertropical Convergence Zone (ITCZ) caused by changes in the Atlantic sea surface temperature gradients. This results in large equatorial precipitation anomalies in the Atlantic, extending into the Pacific and Indian Oceans and affecting precipitation over Central and South America, Africa and south east Asia (Fig. 3 middle). Over much of the northern hemisphere precipitation is decreased, consistent with a cooling-induced decrease in atmospheric moisture content. Other studies have also found a drying over the North Atlantic and a southwards shift of the Atlantic ITCZ (Vellinga and Wood 2002; Stouffer et al. 2006; Kageyama et al. 2012), however the precipitation anomalies over the tropical Pacific and Indian oceans vary substantially between studies. One striking difference in this study is the large drying seen over the Amazon. The large reduction of precipitation over the Amazon occurs in its wet season (DJF) although this is partly compensated by an increase in precipitation in the dry season (JJA). This reduction in seasonality over the Amazon was also seen in Parsons et al. (2014). They found that although the annual mean precipitation decreased over the Amazon (as did the soil moisture and terrestrial water storage), there was actually an increase in primary productivity since the water stress in the dry season was reduced. In this study we find a decrease, rather than increase, of primary productivity (not shown) which might be explained by the greater decrease in precipitation found here.

4 Impacts on Europe

The climate of Europe, particularly western Europe, is significantly influenced by Atlantic sea temperature due to the prevailing westerly weather systems. Hence, large temperature decreases over the Atlantic ocean have widespread impacts throughout Europe.

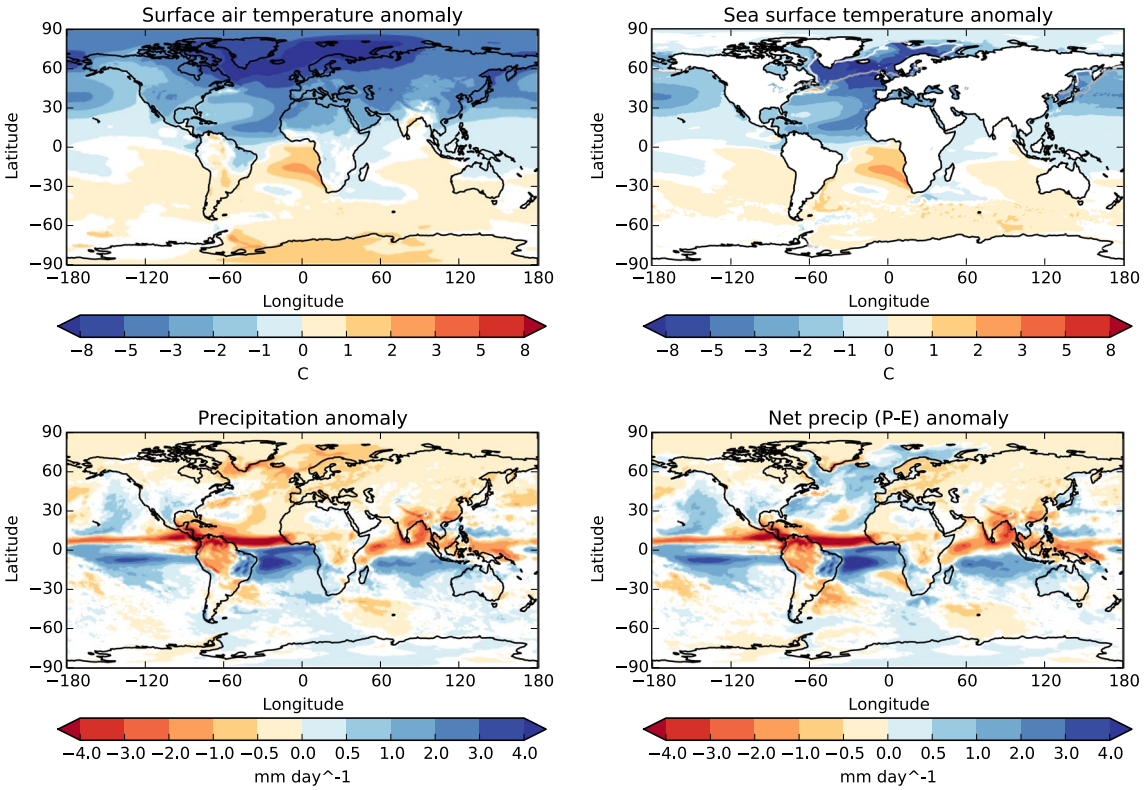

Fig. 3 Anomalies of surface air temperature (*top left*, °C), sea surface temperature (*top right*, °C), precipitation (*bottom left*, mm/day) and net precipitation (precipitation–evapotranspiration) (*bottom right*, mm/day). Anomalies that are not significant compared to the control variability (see text) are *white*. The *top right panel* also shows the extent of the March sea ice (concentrations >15 %) for the control (*white lines*) and perturbed experiment (*grey lines*)

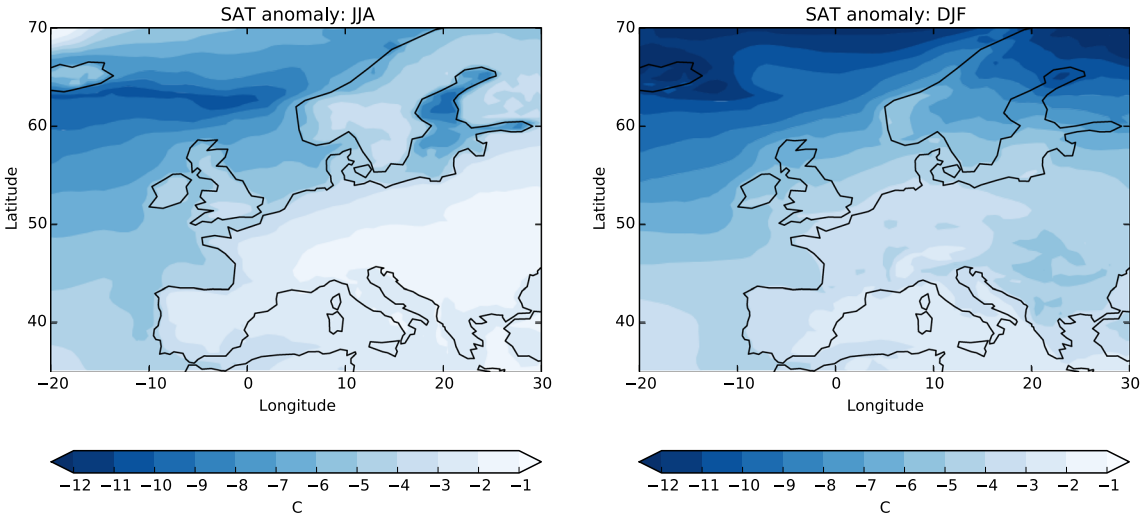

Fig. 4 Surface air temperature anomaly over Europe in season JJA (*left*) and DJF (*right*) in °C. Anomalies at all grid points shown are significant compared to the control variability (see text)

4.1 Cooling

Europe experiences widespread cooling when the AMOC is reduced (Fig. 4) with the greatest cooling in the far north of Europe in winter which appears to be greatly affected by the amplified winter cooling in the Arctic, with temperature decreases in excess of 10 °C. Western Europe shows a more uniform cooling year round. These results are consistent

with previous studies that have mainly shown cooling over Europe of a few degrees, with the greatest annual mean cooling over western and northern Europe (Vellinga and Wood 2002, 2008; Jacob et al. 2005; Laurian et al. 2010). One exception is Kuhlbrodt et al. (2009) who found little cooling over northern Europe when using a downscaling technique to give regional projections on a finer resolution (0.5° × 0.5°) from a coarse resolution global climate model. This result may be a consequence of their downscaling technique since their global model shows wide scale cooling over the whole region. Generally cooling over land is less than at similar latitudes over the ocean, with the exception of eastern Europe in winter. The greater cooling of surface air temperature over the ocean is to be expected because of the large reduction in surface heat flux out of the ocean, consistent with a large reduction of meridional ocean heat transport (Fig. 2). However the European land mass is strongly affected by the marine climate and several factors that might affect the land-sea contrast in the cooling pattern are discussed below.

Laurian et al. (2010) propose that the land–sea contrast in the cooling pattern is maintained by changes in cloud cover. They find that the oceanic cooling causes a more stable marine boundary layer and more low clouds over the ocean [see also Klein and Hartmann (1993)]. They also show that there is reduced transport of moisture from the ocean to the land resulting in a decrease in clouds over land. Consistent with Laurian et al. (2010), in the annual mean we see an increase in cloud over the ocean and a reduction over land (Fig. 5f). This results in radiative changes at the top-of-atmosphere (TOA), with the spatial pattern of the cloud radiative changes being dominated by the shortwave (rather than longwave) component (Fig. 5b, d), suggesting that it is primarily driven by changes in low-level cloud. These changes in the cloud radiative components of the TOA flux generally warm the land and cool the ocean. The land-sea contrast in the cloud forcing is opposed by that in the clear sky (no cloud) radiative components. Over land there is an increase in surface albedo due to increased snow cover (Fig. 10) which was also seen by Jacob et al. (2005), resulting in more reflected shortwave radiation, and a cooling. This mitigates the shortwave warming over land resulting from the reduction in cloud and reduces the land-sea contrast in the total shortwave radiative component (Fig. 5c). There is also less outgoing longwave clear sky radiation, particularly over the ocean, since the ocean has cooled more (Fig. 5a). Hence the net (shortwave + longwave) TOA radiation balance shows no consistent contrast between the changing fluxes over land and ocean (Fig. 5e).

There are also important seasonal variations in these changes. Cloud and albedo changes in winter (Fig. 5h) are similar to those in the annual mean, although the albedo changes dominate the net TOA flux leading to a net cooling over land (not shown). In summer the cloud changes are different (Fig. 5g), with increased cloud over southern Europe and reduced cloud over northern Europe. There is still a relative increase in cloud over ocean compared to that over the land, however. Greater solar insolation leads to an enhancement of the shortwave cloud radiative effect and hence the cloud changes dominate the radiative impact in summer (not shown).

Another process that can affect the constrast in land-ocean temperature changes is the change in thermal advection to continental Europe. Colder ocean temperatures would suggest that this advection should have a net cooling effect, however the change in advection will also be affected by changing wind patterns. In winter there is a strengthening of the southwesterly winds and in summer a weakening. This is consistent with changes in sea level pressure (SLP) shown in Fig. 8 and discussed further in Sect. 4.2.

The change in thermal advection between the perturbed and control experiment shows anomalous warming over land in both summer and winter (Fig. 6; see "Appendix" for definition). In winter the predominantly southwesterly winds normally have a warming effect on Europe since the ocean is warmer than the land. When the AMOC is weak, although the ocean cools more than the land, the ocean is still warmer than the land in absolute terms, so the increase in southwesterly winds acts to warm Europe. In summer the southwesterly winds normally have a cooling effect on Europe since the land is warmer than the sea. When the AMOC is weak this temperature gradient is stronger, but there is also a weakening of the westerly winds. The net effect is a relative warming.

Although the changes in seasonal mean thermal advection suggest a warming in both seasons, the total thermal advection is complex and also depends on high frequency wind fluctations. Periods of time where the wind is not from the prevailing southwesterly direction will also have an impact on temperatures: particularly when the wind is from the much colder north. The importance of changes in thermal advection to the actual surface temperature change also needs to be demonstrated. To show how advection from the prevailing winds affects European surface temperature (T_S), a regression model was built between area averaged T_S and seasonal mean advection at 850 hPa (see "Appendix"). This gives significant correlations of 0.5–0.7 for central European regions giving us confidence in the importance of the seasonal mean advection. This regression model can also be used to separate the changes in thermal advection from temperature changes and wind changes. Applying the regression model developed between thermal advection and T_S to the advection calculated with no wind changes (using winds from the control experiment) suggests that the cooling over Europe in the absence of the

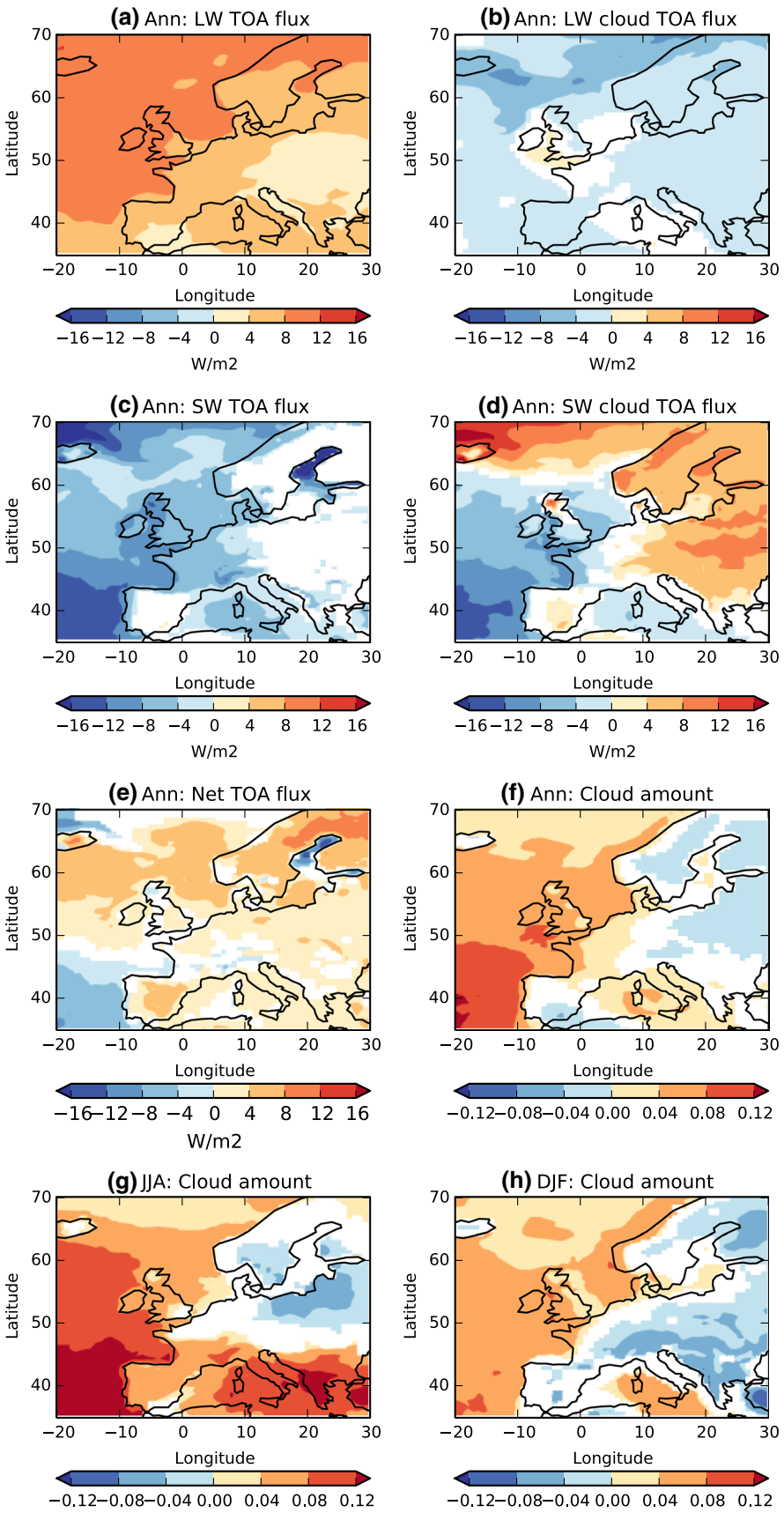

Fig. 5 Anomalous TOA radiative fluxes and cloud fractions. *Top left* annual mean longwave flux. Positive values indicate net energy flux downwards (W/m^2). *Top right* cloud component of annual mean longwave flux (W/m^2). *Second row left* annual mean shortwave flux. (W/m^2). *Second row right* cloud component of annual mean shortwave flux (W/m^2). *Third row left* annual mean net flux (W/m^2). *Third row right* anomaly in annual mean cloud fraction. *Bottom row* anomaly in JJA (*left*) and DJF (*right*) cloud fraction. Anomalies that are not significant compared to the control variability (see text) are *white*

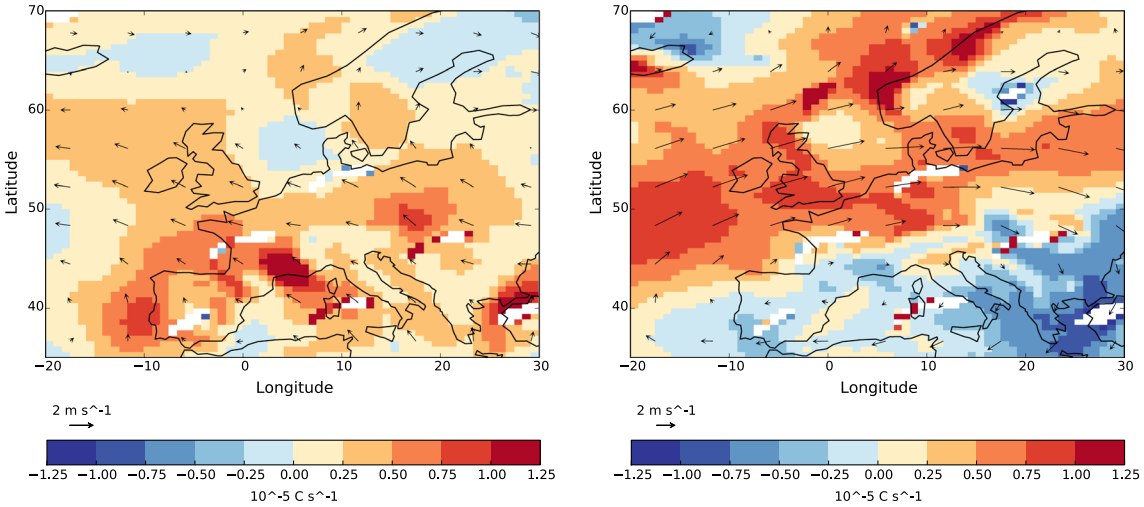

Fig. 6 Anomalies in thermal advection ($-u.\nabla T$) at 850 hPa (10^{-5} °C s^{-1}) as contours for JJA (*left*) and DJF (*right*). Positive values indicate a warming by the advection. Overlain are the anomalous wind vectors

wind response would be of order 10–30 % stronger. Hence the atmospheric circulation changes result in a reduction in the cooling over land in Europe.

4.2 Precipitation and weather patterns

The high horizontal resolution in this study reveals specific features such as enhanced precipitation over topographical features and western coasts (Fig. 7), suggesting that we can have greater confidence in regional and local projections. When the AMOC is reduced there is a general reduction in precipitation over Europe as colder temperatures reduce the amount of water that is held in the atmosphere, however there are also local changes in precipitation that are likely caused by changes in atmospheric circulation.

Summer precipitation changes show a clear distinction between the Mediterranean, which becomes wetter, and northern Europe, which becomes drier. Vellinga and Wood (2002) and Jacob et al. (2005) report drying in both seasons across Europe, although in Vellinga and Wood (2008) there is some signal of increased annual mean precipitation over the Mediterranean sea, but not land. It should be noted that the increase in precipitation in the Mediterranean in both this study and that of Vellinga and Wood (2008) is small in absolute terms (about 0.5 mm/day) although this can mean an increase of about 35 % in summer rainfall. These regional changes can be contrasted with projected changes in future scenarios with increased CO_2 where summer rainfall is predicted to decrease across Europe (Collins et al. 2013). Hence precipitation changes associated with a large AMOC reduction could be expected to reinforce the drying over northern Europe and oppose the drying over southern Europe.

The different responses for northern Europe and the Mediterranean resemble the observational findings of Sutton and Dong (2012). They found increased (decreased) summer precipitation over northern Europe (the Mediterranean) associated with warm surface Atlantic temperatures during years with a positive Atlantic Multidecadal Oscillation (AMO) index. They attribute their patterns to a positive summer North Atlantic Oscillation (NAO) pattern (Folland et al. 2009) with anomalously low sea level pressure over the UK. Since our experiment has anomalously cold, rather than warm, surface temperatures over the Atlantic we find the signal with the signs reversed: decreased (increased) precipitation over northern Europe (the Mediterranean). Also consistent with the Sutton and Dong (2012) findings is an anomalous high pressure signal over the UK and Scandinavia in summer resulting in a negative summer NAO (Fig. 8 left). Magnitudes of both the precipitation and pressure anomalies are of similar size to those found in observations by Sutton and Dong (2012), although the sea surface temperature (SST) changes in the Atlantic are 5–10 times larger in this study. Other studies have also suggested that the atmosphere responds too weakly to North Atlantic sea surface temperatures in models (Gastineau et al. 2013; Scaife et al. 2014), although a stronger response has been found in models with higher resolution (Minobe et al. 2008; Kirtman et al. 2012). This suggests that the magnitude of the summer precipitation response to Atlantic cooling could be much larger.

In winter there is a general drying over Europe apart from over few localised regions, in particular western coasts of the UK and Norway. These regions are affected by a strengthening and eastwards extension of the winter storm track [measured by the variance of filtered 6 hourly

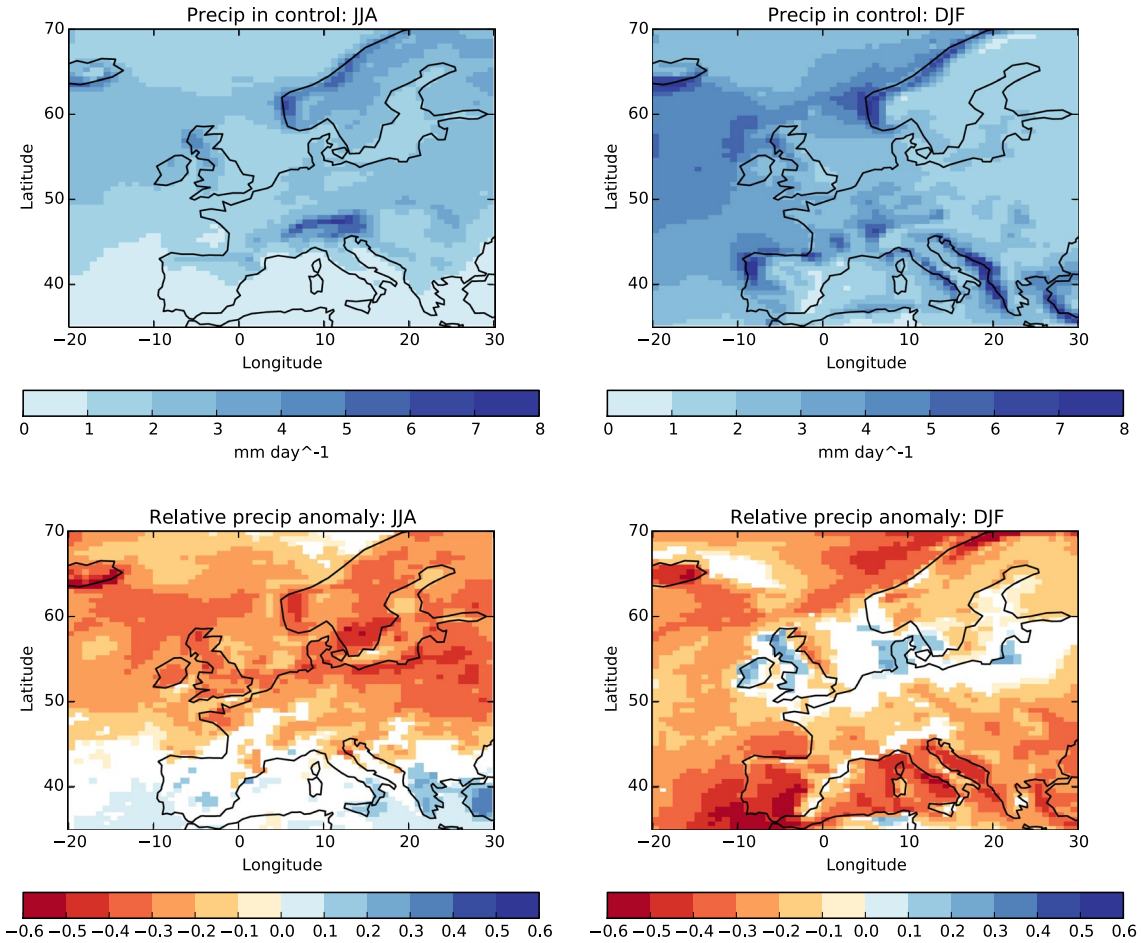

Fig. 7 Precipitation in the control (*top*) and anomalies in the perturbation experiment (*bottom*) for JJA (*left*) and DJF (*right*) over Europe. Precipitation is measured in mm/day in the *top* panels and shown as a relative or fractional change in the *bottom* panels. Anomalies that are not significant compared to the control variability (see text) are *white*

winter SLP, as in Brayshaw et al. (2009)] shown in Fig. 9. Although there is less water content in the atmosphere, the intensification of the storm track implies more and/or more intense winter storms resulting in localised increases in precipitation where the storms make landfall. This strengthened storm track also results in an increase in mean winter wind speed along its path (Fig. 9, bottom right) with increases of 10–20 % over land.

Brayshaw et al. (2009) similarly found an increase in strength and eastwards penetration of the storm track in an experiment with a weakened AMOC. They find that these changes in the storm track are caused by a strengthening of the SST gradients over the northern Atlantic (as the subpolar gyre cools more than the subtropics) which increases the baroclinicity of the near surface atmosphere. Associated with this strengthening of the storm track we see a strengthening of the Azores high which projects onto the winter NAO pattern resulting in a shift to a more positive winter NAO (Fig. 8 bottom right). There is also evidence from both observations and models of a consistent relationship between multidecadal Atlantic cooling variations and the positive NAO, especially reflecting a strengthening of the Atlantic jet (Peings and Magnusdottir 2014; Woollings et al. 2014).

The wintertime upper tropospheric circulation response is almost identical to that in Fig. 5 of Brayshaw et al. (2009), so is not shown here. This response comprises a strengthening of both the eddy-driven jet at about 55°N and the subtropical jet at about 25°N, enhancing the split jet structure over the eastern North Atlantic. As in Brayshaw et al the meridional wind shows that the strengthened subtropical jet is driven by a local enhancement of the Hadley Cell over the tropical SST anomalies. The strengthening of the eddy-driven jet is consistent with the increase in baroclinicity, and hence storm activity over the mid-latitude SST anomalies. There is potential for the tropical SST anomalies to have an additional influence on the eddy-driven jet, however further experiments would be needed to

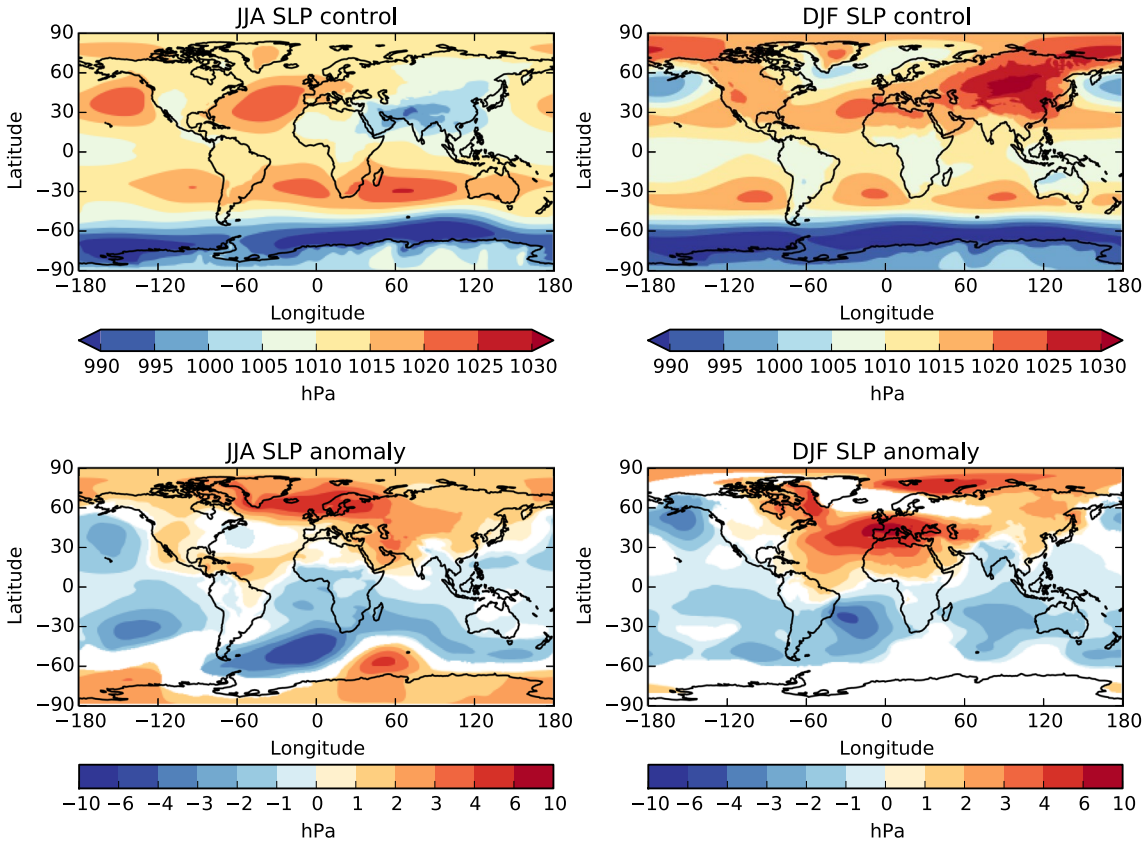

Fig. 8 Sea Level Pressure (SLP) in the control (*top*) and anomalies in the perturbed experiment (*bottom*) for seasons DJF (*left*) and JJA (*right*). Units are hPa. Anomalies that are not significant compared to the control variability (see text) are *white*

investigate this. In summer (JJA) the subtropical response is similar to winter but in the extratropics the eddy-driven jet shifts to the north rather than strengthening.

Projections of winter precipitation change under increasing CO_2 show increased precipitation over northern Europe and reduced precipitation over southern Europe (Collins et al. 2013). In a scenario with an additional strong decrease of the AMOC we might then expect the precipitation patterns associated with the AMOC decrease to oppose the increased precipitation in northern Europe, apart from on western coasts, and reinforce the drying across southern Europe.

The rate of snowfall increases in most regions and seasons, despite the decrease in total precipitation, and the proportion of precipitation falling as snow increases everywhere. SON (Fig. 10 top left) and JJA (not shown) show increased rates of snowfall everywhere, though in the latter these are still very small. In DJF (Fig. 10 top right) and MAM (not shown) there is an increase in snowfall rates over western Europe and particularly along the path of the strengthened storm track where rates nearly double over Western Scotland and Norway. Parts of Scandinavia and Eastern Europe show decreased snowfall. The increased snowfall, particularly in SON and MAM indicates a prolonged snowy season that starts earlier and finishes later in the year. This might be expected for a colder climate and has been noted in previous studies (Vellinga and Wood 2008; Jacob et al. 2005). There is also an increase in snow depth everywhere and an increase in the number of months with significant snow cover (depth >5 cm). In particular central Europe and Scotland experience a large increase in the length of the season with snow cover (Fig. 10 bottom).

4.3 Rivers and surface runoff

The cooling and drying over Europe and the change into a more snowy regime lead to a clear and consistent reduction in surface runoff and river flow across Europe (Figs. 11, 12). The runoff anomaly maps reflect the spatial pattern of changes to the hydrological cycle, while the river flows enable us to examine the changes over an entire river basin. Changes to river flows in southern European rivers mainly reflect the direct rainfall, while in northern and Eastern Europe they are also driven by changes to snowmelt amount and timing. The large-scale decrease in runoff is most pronounced in winter (Fig. 11a). In summer, however,

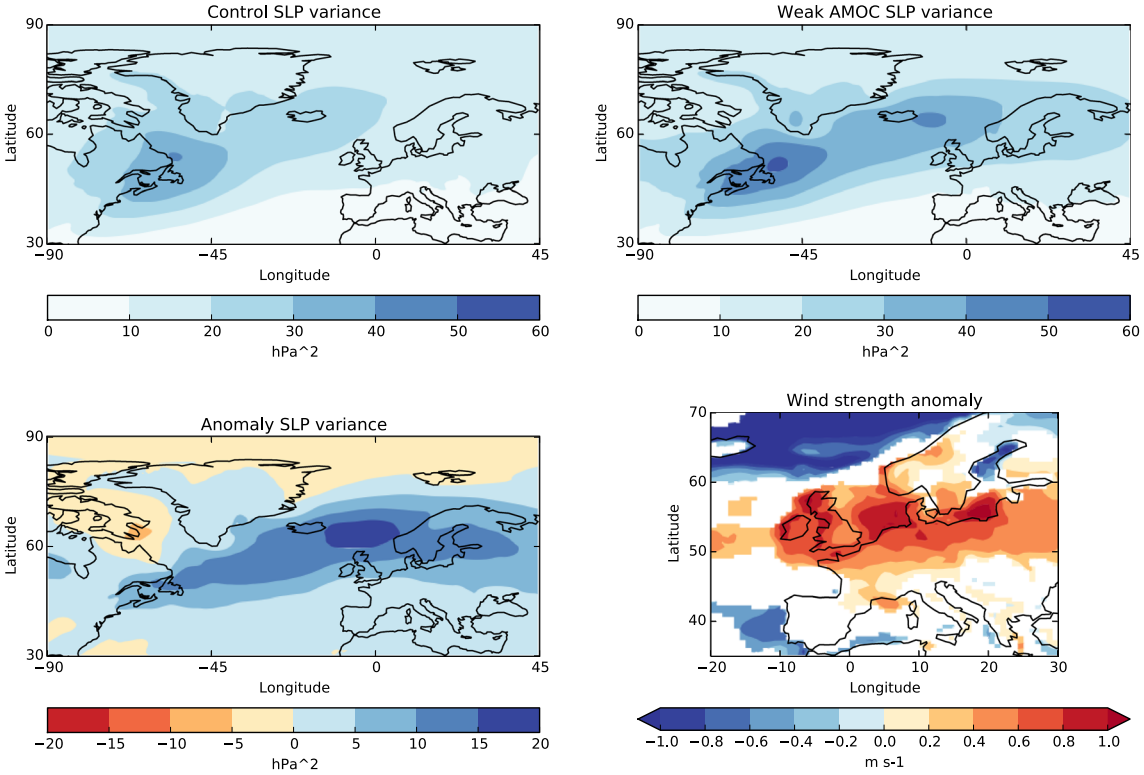

Fig. 9 Winter storm tracks in the control (*top left*), perturbed experiment (*top right*) and anomalies (perturbed-control) (*bottom left*). These are measured as the variance of 6 hourly winter SLP after a 2–6 day band pass filter. Units are hPa^2. Also shown is the anomalous winter wind speed (ms^{-1}, *bottom right*)

runoff increases in southern Europe and the Mediterranean (consistent with the seasonal precipitation changes shown in Fig. 7) and in northern Europe, where it might indicate a snowmelt peak later in the season.

The long-term average monthly flow for the Garonne and the Danube rivers is shown in Fig. 12a, b. We have extracted the simulated river flows for the control and the perturbed experiments from grid cells adjacent to river gauges that represent, as much as possible, the entire basin, and present it along with the observational data from GRDC river gauges (GRDC). The model captures the flow reasonably well but does not always reproduce the seasonality or the variability of the observations, possibly due to the relatively coarse model resolution as well as human interventions to the natural flow by means of dams and irrigation. Changes to the flow in the Garonne in Southern France are typical for rivers in western Europe and show a decrease of the winter high flow of about 30 %. The maximum flow in early spring is shifted from March to April and the differences in low flow during late-summer are smaller, suggesting a less pronounced seasonal cycle of the flow. The considerable decrease in discharge is typical for large rivers throughout Europe, and the stronger decrease in winter is more pronounced in rivers in southwest Europe. For example, rivers In the Iberian peninsula show very strong decreases (up to 80 %) of predicted winter high flow while late summer low flow values decreased only by 0–30 %. This is consistent with the pattern of precipitation change in southern Europe (Fig. 7).

Rivers in central and eastern Europe show a more uniform reduction of river flow under a weaker AMOC climate (Fig. 12b) and in some, both the high and weak flows are shifted forward by a month. The magnitude of flow reduction (30–80 %) is comparable, if not larger than changes predicted under the most severe projections of future climate change (Milly et al. 2005; Falloon and Betts 2006; Hurkmans et al. 2010). Future climate change simulations predict an annual increase in runoff in northern Europe, mostly in winter and earlier spring due to earlier snowmelt (Falloon and Betts 2010). A weakened AMOC, however, results in a decreased flow throughout Europe, which can have implications for natural systems and a range of human activities.

4.4 Vegetation

The AMOC weakening causes a strong reduction in plant productivity across the northern hemisphere. The decrease

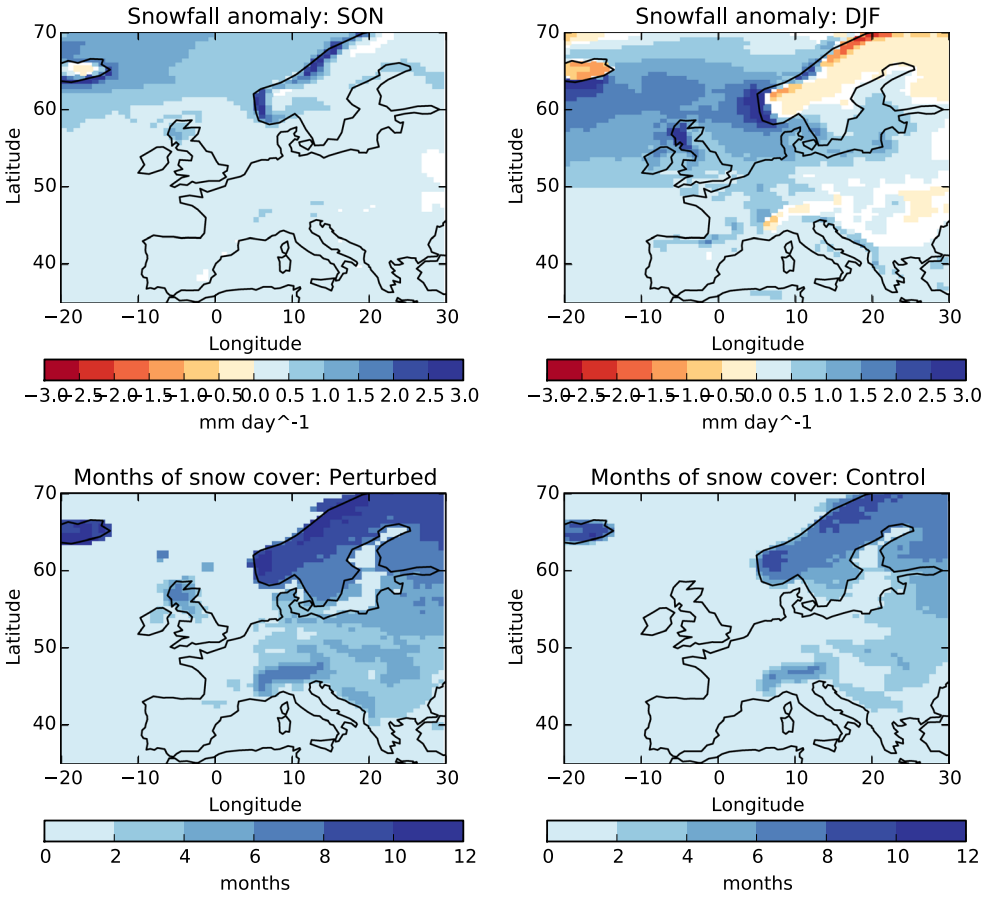

Fig. 10 *Top panels* show anomalies of snowfall rates (mm/day) over Europe and the North Atlantic for SON (*left*) and DJF (*right*). *Bottom* panels show the average number of months with a snow cover of greater than 5 cm for the perturbed (*left*) and control (*right*) experiments

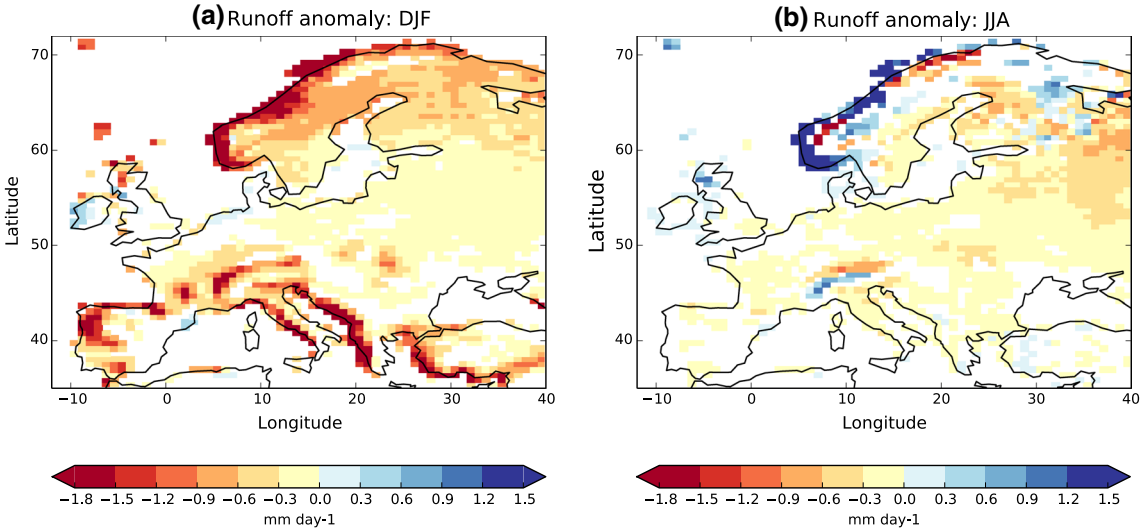

Fig. 11 Runoff anomalies between the perturbed and the control simulations for DJF (*left*) and JJA (*right*). Anomalies that are not significant compared to the control variability (see text) are *white*

is most pronounced in high latitudes (>50°N) and in the growing season (spring and summer). The decrease of Net Primary Productivity (NPP) due to the colder and drier conditions over Europe is shown in Fig. 13 and generally follows regional patterns of change to the net precipitation (precipitation–evapotranspiration, Fig. 3).

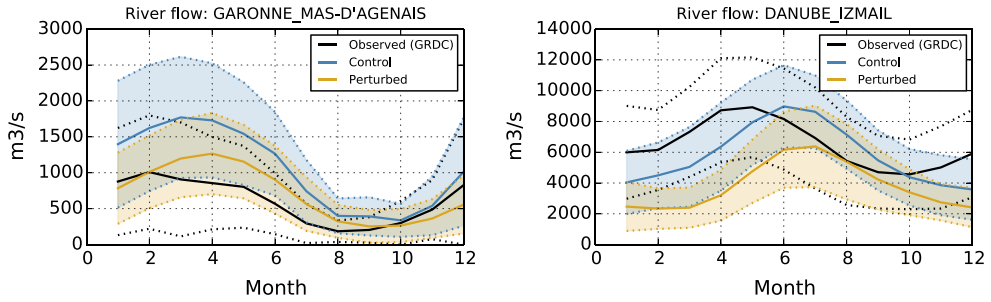

Fig. 12 Monthly river flow ($m^3\ s^{-1}$) for the Garonne (*left*) and the Danube (*right*) for the control (*blue*) and perturbed (*orange*) experiments. Simulated river flow is from the grid cell closest to available historical river gauges data from GRDC (*black lines*). The modelled river flow annual cycle is calculated over 30 years and the *shaded areas* and *dashed black lines* reflect one standard deviation

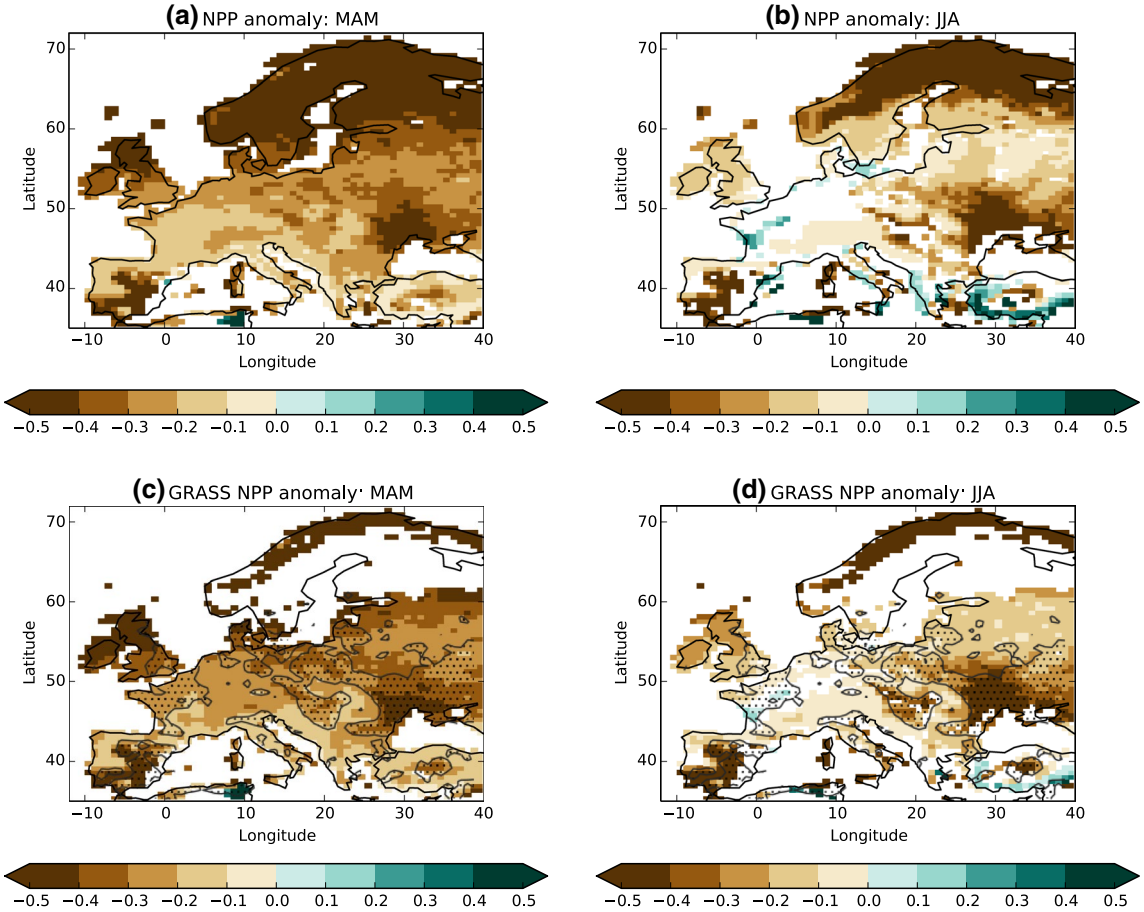

Fig. 13 Relative fractional changes to net primary productivity (NPP) between the perturbed run and the control. Spring (MAM, panel **a**) and Summer (JJA, panel **b**) NPP anomaly for total vegatation. **c** and **d** Same as **a** and **b** but for grasses only. *Dotted areas* in **c** and **d** are regions where present day cropland is large that 40 % Ramankutty et al. (2008). Anomalies that are not significant compared to the control variability (see text) are *white*

The decline in plant productivity is marked over western Europe temperate forest regions in spring and over higher latitude boreal forest regions in summer (Fig. 13a, b). The model is capable of separating NPP of different types of vegetation (not shown) and shows that under the 'weakened AMOC' climate regime there are substantial (30–50 %) reductions in productivity of broadleaf forests in the Baltic and Mediterranean, and needleleaf forests in northern Europe. There is an increase in summer productivity, of about 10–40 % along parts of the north Mediterranean coast

in Turkey and Greece, (associated mainly with shrubs), and a small (<30 %) increase in summer productivity of grasses and shrubs in France (Fig. 13a, b). Plants in these regions might have benefitted from the marked decreases in evapotranspiration and increases in precipitation.

Lower productivity of land vegetation at the time of reduced AMOC was found in Zickfeld et al. (2008) and Vellinga and Wood (2002) and for some regions in Kuhlbrodt et al. (2009) (see their Fig. 10). Plant productivity reductions over Europe in this experiment are much more uniform and an order of magnitude larger then those in Kuhlbrodt et al. (2009) which is consistent with the smaller cooling and spatially variable precipitation changes they present. The scenario they used included much higher levels of CO_2 which enhanced plant productivity and dominated any effect from the AMOC weakening. The direct CO_2 fertilisation effect was shown by Falloon and Betts (2010) and Wiltshire et al. (2013) to increase plant productivity under CO_2-induced future climate change scenarios and is not modelled here.

Our estimated annual vegetation productivity decrease over Europe is somewhat larger than the 0.9 Gt Carbon per year (about 16 % decrease) found by Vellinga and Wood (2002). We estimate an annual decrease of 3.7 Gt C or a reduction of 26 % in primary productivity over Europe. These larger reductions are consistent with a stronger magnitude of change in most other parameters examined here and are likely to be a response to the greater cooling found in this study (see Sect. 4.1)

4.4.1 Possible effects on food production

To identify possible impacts on agricultural productivity and crop yield, we examine the changes in productivity of the model's temperate and tropical (C3 and C4) grasses in main agricultural areas [defined by Ramankutty et al. (2008)] as a crude measure of crop yield. This approach enables us to estimate only the large-scale response in European major cropland areas and does not include important agricultural aspects such as irrigation, pests control or diseases [see a fuller discussion in Wiltshire et al. (2013)]. Furthermore, the ecosystem changes shown here are only related to changes in the hydrological cycle and temperature changes, and do not include direct CO_2 effects.

Crop productivity in the main agricultural regions in western Europe (Spain, France and Germany), the UK and northern Europe (most notably Denmark) and in central and eastern Europe (Poland and Ukraine) decreases dramatically. This decline is probably due to the combined effect of colder temperatures and water stress caused by changes in the water cycle. The lower productivity is marked in spring, when we find an overall drying and very small or no reduction to the evapotranspiration rates (Fig. 13c). However, there is also a strong reduction in summer crop productivity in eastern Europe and mainly around the Black sea (Bulgaria, Romania, Ukraine), where agriculture is currently an important part of the economy (Fig. 13d).

Grass productivity in main grazing regions is also reduced in spring and summer by up to 50 % in Ireland and western UK and to a lower degree (10–20 %) in mountain ranges from the Carpathians and Balkans in the east through to the Alps, the Pyrenees and the Iberian mountains in the west.

The strong reduction of crop yield and pasture over Europe in a 'weakened AMOC' climate regime is consistent with the strong cooling and drying. The decrease is stronger in the north but all regions will become less attractive for cropland than today. Globally, however, we found enhanced grass productivity in the southern hemisphere and areas in Australia, southern Africa and eastern Brazil that might become potentially suitable for crops.

Simulations of crop productivity under future (CO_2 -induced) climate change scenarios show a similar decrease for the Mediterranean, due to the warming and drying of this region. In northern Europe, however, crop productivity is shown to increase, with cropland extending further northwards, both because of the direct fertilisation effect of the higher atmospheric CO_2 concentration and because of the annual temperature increase that might lead to a longer growing season (Falloon and Betts 2010).

5 Conclusions

We have assessed the impacts to climate from a collapse of the Atlantic Meridional Overturning Circulation (AMOC) using the Met Office Hadley Centre's most recent global climate model (GCM) HadGEM3, with particular focus on the impacts in Europe. This is a state-of-the-art climate model and is the highest resolution model used for such a study.

Many results found are consistent with previous studies and can be considered robust impacts from a large reduction or collapse of the AMOC. These include:

- Widespread cooling throughout the North Atlantic and northern hemisphere in general, with cooling in Europe of several degrees.
- Much greater sea ice coverage in the North Atlantic.
- Less precipitation and evaporation in the northern hemisphere mid-latitudes.
- Large changes in precipitation in the tropics with a southwards shift of the Atlantic Intertropical Convergence Zone.
- A strengthening of the North Atlantic storm tracks.

- The focus on Europe and increased resolution has revealed new impacts that have previously not been discussed. The most significant are:

- Summer precipitation decreases across much of Europe, however there is an increase in precipitation around the Mediterranean. This pattern is associated with a negative summer NAO.
- In winter, the storm tracks across the North Atlantic and into Europe are strengthened and penetrate further over land (as seen before). The higher resolution of this model enables us to see very localised regions of increased precipitation likely caused by the increase in winter storms, despite the general signal of decreased winter precipitation across Europe.
- Greater proportion of precipitation falling as snow over all Europe. There is also an increase in the number of months with significant snow cover.
- In both winter and summer the atmospheric circulation response moderates the cooling over central Europe: in winter the westerly winds strengthen, enhancing the winter maritime warming effect, while in summer the westerly winds weaken, which weakens the summer maritime cooling effect. The cooling over Europe is also moderated by reduced cloud cover over land that allows more shortwave radiation to reach the surface, but this is offset by increased albedo from greater coverage of snow and ice.
- River flow and surface water runoff in Europe are significantly reduced because of the reduction in precipitation, however they are also affected by the distribution of precipitation changes and changes to the snowmelt timing.
- Vegetation and crop productivity show strong decreases over Europe in response to the cooling and decrease in available water.

- Many of these new results are associated with changes in the atmospheric circulation and might be model dependent, however the general patterns of change found here are supported by previous studies, including evidence from observational records. A summer NAO pattern in the sea level pressure has previously been associated with changes in sea surface temperature of the North Atlantic, and has been linked to a similar pattern of precipitation change as found in this study (Sutton and Dong 2012; Folland et al. 2009). A negative summer NAO signal would also be expected to weaken the prevailing westerly winds over Europe. Likewise, changes in winter sea level pressure have also previously been associated with changes in North Atlantic sea temperatures, with colder temperatures and stronger temperature gradients producing a positive NAO pattern (Peings and Magnusdottir 2014) (resulting in stronger westerly winds) and a strengthening of the North Atlantic storm track (Brayshaw et al. 2009). Hence the patterns of response found here to a weakened AMOC are plausible, although there are suggestions that the magnitudes of response might be stronger in a reality (Kirtman et al. 2012; Scaife et al. 2014).

The consequences of an AMOC collapse and the potential impacts on human and natural systems are very large and would affect not only Europe but large regions across the globe. The 5th Intergovernmental Panel on Climate Change has assessed a complete collapse of the AMOC to be very unlikely within the 21st century, however a weakening of the AMOC has been assessed to be very likely (Collins et al. 2013). Even though the likelihood of a collapse is low, the severity of the consequences makes a careful assessment of the impacts expedient.

These results are illustrations of impacts rather than predictions or projections since they are based on an idealised AMOC collapse in a present day climate. If an AMOC reduction occurs in the future, the climatic impacts would be combined with those of increasing greenhouse gases, and would depend on the relative magnitudes and timing of an AMOC reduction and global warming. Many impacts from an AMOC collapse could be of comparable size to, or larger than those from global warming, and although some impacts from global warming would be lessened, others would be reinforced by an AMOC collapse.

Acknowledgments This work was supported by the Joint DECC/Defra Met Office Hadley Centre Climate Programme (GA01101). We would like to thank M. Mizielinski for technical assistance in setting up and running HadGEM3 and C. Mathison and K. Williams for assistance with the river flow analysis. The authors would also like to thank Pete Falloon and Richard Betts for useful discussions during the preparation of this paper. Finally we wish to thank two anonymous reviewers for their comments which improved this manuscript.

Appendix

The thermal advection is calculated as $-\mathbf{u}_{850} \cdot \nabla T_{850}$ using the wind vectors ($\mathbf{u}$) and atmospheric temperatures (T) at 850 hPa. The gradients were calculated as centred differences over 20° in both latitude and longitude to smooth out small scale noise.

To show how advection from the prevailing winds affects European surface temperature (T_S), a regression model was built between seasonal mean T_S and advection at 850 hPa:

$$T_S^p = -A\mathbf{u}_{850}^p \cdot \nabla T_{850}^p + \text{residual}.$$

where T_S^p and $\mathbf{u}_{850}^p \cdot \nabla T_{850}^p$ were area averaged over central European regions showing strong thermal advection changes in Fig. 6 (0–30°E, 50–65°N in DJF and 0–30°E,

45–60°N in JJA). The superscript p indicates that the data were taken from seasonal means from the 30 year period of the perturbation run where the AMOC was reduced in strength, though similar relationships are found in the equivalent 30 year period in the control run. This gives correlations between T_S^p and $-\mathbf{u}_{850}^p \cdot \nabla T_{850}^p$ of 0.5 in DJF and 0.7 in JJA, and values of A of 2.7 $\times$ 10^5s and 1.8 $\times$ 10^5 s respectively. The significant correlations support the importance of the seasonal mean advection in affecting surface temperature.

The cooling associated with the temperature changes alone can be assessed using the regression model above with the wind vector replaced by that from the control experiment:

$$T_S^{p*} = -A\mathbf{u}_{850}^c \cdot \nabla T_{850}^p.$$

Hence the thermal advection is calculated using wind velocities from the control experiment and temperature from the perturbed experiment, effectively assuming the wind field does not change in response to the forcing. Applying this regression model to estimate T_S^{p*} suggests that the cooling over Europe in the absence of the wind response would be 12 % stronger in winter and 34 % stronger in summer. Hence the atmospheric circulation changes result in a reduction in the cooling over land in Europe.

References

Arribas A, Glover M, Maidens A, Peterson K, Gordon M, MacLachlan C, Graham R, Fereday D, Camp J, Scaife AA, Xavier P, McLean P, Colman A, Cusack S (2010) The GloSea4 ensemble prediction system for seasonal forecasting. Mon Weather Rev 139(6):1891–1910. doi:10.1175/2010mwr3615.1

Bernie DJ, Guilyardi E, Madec G, Slingo JM, Woolnough SJ, Cole J (2008) Impact of resolving the diurnal cycle in an ocean atmosphere GCM. Part 2: a diurnally coupled CGCM. Clim Dyn 31(7–8):909–925. doi:10.1007/s00382-008-0429-z

Bitz CM, Lipscomb WH (1999) An energy-conserving thermodynamic model of sea ice. J Geophys Res 104(C7):15,669–15,677. doi:10.1029/1999jc900100

Brayshaw DJ, Woollings T, Vellinga M (2009) Tropical and extratropical responses of the North Atlantic atmospheric circulation to a sustained weakening of the MOC. J Clim 22(11):3146–3155. doi:10.1175/2008jcli2594.1

Bryden HL, Imawaki S (2001) Ocean heat transport. In: Siedler G, Church J, Gould J (eds) Ocean circulation and climate: observing and modelling the global ocean. Academic Press, San Fransisco, pp 455–474

Chang P, Zhang R, Hazeleger W, Wen C, Wan X, Ji L, Haarsma RJ, Breugem WP, Seidel H (2008) Oceanic link between abrupt changes in the North Atlantic Ocean and the African monsoon. Nat Geosci 1(7):444–448. doi:10.1038/ngeo218

Clement AC, Peterson LC (2008) Mechanisms of abrupt climate change of the last glacial period. Rev Geophys 46(4):RG4002+. doi:10.1029/2006rg000204

Collins M, Knutti R, Arblaster J, Dufresne JL, Fichefet T, Friedlingstein P, Gao X, Gutowski WJ, Johns T, Krinner G, Shongwe M, Tebaldi C, Weaver AJ, Wehner M (2013) Long-term climate change: projections, commitments and irreversibility. In: Stocker TF, Qin D, Plattner GK, Tignor M, Allen SK, Boschung J, Nauels A, Xia Y, Bex V, Midgley PM (eds) Climate change 2013: the physical science basis. Contribution of working group I to the fifth assessment report of the intergovernmental panel on climate change. Cambridge University Press, Cambridge

Demory ME, Vidale P, Roberts M, Berrisford P, Strachan J, Schiemann R, Mizielinski M (2013) The role of horizontal resolution in simulating drivers of the global hydrological cycle. Clim Dyn 1–25: doi:10.1007/s00382-013-1924-4

de Vries P, Weber SL (2005) The Atlantic freshwater budget as a diagnostic for the existence of a stable shut down of the meridional overturning circulation. Geophys Res Lett 32:L09606. doi:10.1029/2004GL021450

Drijfhout S, van Oldenborgh GJ, Cimatoribus A (2012) Is a decline of AMOC causing the warming hole above the North Atlantic in observed and modeled warming patterns? J Clim 25(24):8373–8379. doi:10.1175/jcli-d-12-00490.1

Falloon PD, Betts RA (2006) The impact of climate change on global river flow in HadGEM1 simulations. Atmos Sci Lett 7(3):62–68. doi:10.1002/asl.133

Falloon P, Betts R (2010) Climate impacts on European agriculture and water management in the context of adaptation and mitigation the importance of an integrated approach. Sci Total Environ 408(23):5667–5687. doi:10.1016/j.scitotenv.2009.05.002

Folland CK, Knight J, Linderholm HW, Fereday D, Ineson S, Hurrell JW (2009) The summer North Atlantic Oscillation: past, present, and future. J Clim 22(5):1082–1103. doi:10.1175/2008jcli2459.1

Gaspar P, Grégoris Y, Lefevre JM (1990) A simple eddy kinetic energy model for simulations of the oceanic vertical mixing: tests at station Papa and Long-Term Upper Ocean Study site. J Geophys Res 95(C9):16,179–16,193. doi:10.1029/jc095ic09p16179

Gastineau G, D'Andrea F, Frankignoul C (2013) Atmospheric response to the North Atlantic Ocean variability on seasonal to decadal time scales. Clim Dyn 40(9–10):2311–2330. doi:10.1007/s00382-012-1333-0

Gent PR, Mcwilliams JC (1990) Isopycnal mixing in ocean circulation models. J Phys Oceanogr 20(1):150–155. doi:10.1175/1520-0485(1990)020<0150:imiocm>2.0.co;2

Good P, Lowe JA, Andrews T, Wiltshire A, Chadwick R, Ridley JK, Menary MB, Bouttes N (2015) Nonlinear regional warming with increasing CO2 concentrations. Nat Clim Chang 5.2:138–142

Hemming D, Betts R, Collins M (2013) Sensitivity and uncertainty of modelled terrestrial net primary productivity to doubled CO2 and associated climate change for a relatively large perturbed physics ensemble. Agric For Meteorol 170:79–88. doi:10.1016/j.agrformet.2011.10.016

Hewitt HT, Copsey D, Culverwell ID, Harris CM, Hill RSR, Keen AB, McLaren AJ, Hunke EC (2011) Design and implementation of the infrastructure of HadGEM3: the next-generation Met Office climate modelling system. Geosci Model Dev 4(2):223–253. doi:10.5194/gmd-4-223-2011

Hunke EC, Lipscomb WH (2010) CICE: the Los Alamos Sea Ice Model, documentation and software user's manual. Version 4.1. Technical report LA-CC- 06-012, Los Alamos National Laboratory, Los Alamos, New Mexico. http://oceans11.lanl.gov/trac/CICE. Last access 6 Feb 2014

Hurkmans R, Terink W, Uijlenhoet R, Torfs P, Jacob D, Troch PA (2010) Changes in streamflow dynamics in the Rhine basin under three high-resolution regional climate scenarios. J Clim 23(3):679–699. doi:10.1175/2009jcli3066.1

Ineson S, Scaife AA (2009) The role of the stratosphere in the European climate response to El Nino. Nat Geosci 2(1):32–36. doi:10.1038/ngeo381

Jackson LC (2013) Shutdown and recovery of the AMOC in a coupled global climate model: the role of the advective feedback. Geophys Res Lett 40:1182–1188. doi:10.1002/grl.50289

Jacob D, Goettel H, Jungclaus J, Muskulus M, Podzun R, Marotzke J (2005) Slowdown of the thermohaline circulation causes enhanced maritime climate influence and snow cover over Europe. Geophys Res Lett 32(21):L21,711+. doi:10.1029/2005gl023286

Kageyama M, Merkel U, Otto-Bliesner B, Prange M, Abe-Ouchi A, Lohmann G, Roche DM, Singarayer J, Swingedouw D, Zhang X (2012) Climatic impacts of fresh water hosing under Last Glacial Maximum conditions: a multi-model study. Clim Past Discuss 8(4):3831–3869. doi:10.5194/cpd-8-3831-2012

Kirtman B, Bitz C, Bryan F, Collins W, Dennis J, Hearn N, Kinter J, Loft R, Rousset C, Siqueira L, Stan C, Tomas R, Vertenstein M (2012) Impact of ocean model resolution on CCSM climate simulations. Clim Dyn 39(6):1303–1328. doi:10.1007/s00382-012-1500-3

Klein SA, Hartmann DL (1993) The seasonal cycle of low stratiform clouds. J Clim 6(8):1587–1606. doi:10.1175/1520-0442(1993)006<1587:tscols>2.0.co;2

Kuhlbrodt T, Rahmstorf S, Zickfeld K, Vikebø F, Sundby S, Hofmann M, Link P, Bondeau A, Cramer W, Jaeger C (2009) An integrated assessment of changes in the thermohaline circulation. Clim Change 96(4):489–537. doi:10.1007/s10584-009-9561-y

Laurian A, Drijfhout SS, Hazeleger W, Hurk B (2010) Response of the Western European climate to a collapse of the thermohaline circulation. Clim Dyn 34(5):689–697. doi:10.1007/s00382-008-0513-4

Levermann A, Griesel A, Hofmann M, Montoya M, Rahmstorf S (2005) Dynamic sea level changes following changes in the thermohaline circulation. Clim Dyn 24(4):347–354. doi:10.1007/s00382-004-0505-y

Madec G (2008) NEMO ocean engine, Note du Pole de modèlisation. France, no 27. ISSN No 1288–1619

Manabe S, Stouffer RJ (1997) Coupled ocean–atmosphere model response to freshwater input: Comparison to Younger Dryas event. Paleoceanography 12(2):321–336. doi:10.1029/96pa03932

Megann A, Storkey D, Aksenov Y, Alderson S, Calvert D, Graham T, Hyder P, Siddorn J, Sinha B (2013) Go5.0: the joint NERC-Met Office NEMO global ocean model for use in coupled and forced applications. Geosci Model Dev Discuss 6(4):5747–5799. doi:10.5194/gmdd-6-5747-2013

Milly PCD, Dunne KA, Vecchia AV (2005) Global pattern of trends in streamflow and water availability in a changing climate. Nature 438(7066):347–350. doi:10.1038/nature04312

Minobe S, Kuwano-Yoshida A, Komori N, Xie SP, Small RJ (2008) Influence of the Gulf Stream on the troposphere. Nature 452(7184):206–209. doi:10.1038/nature06690

Parsons LA, Yin J, Overpeck JT, Stouffer RJ, Malyshev S (2014) Influence of the atlantic meridional overturning circulation on the monsoon rainfall and carbon balance of the American tropics. Geophys Res Lett 41(1):2013GL058,454+. doi:10.1002/2013gl058454

Peings Y, Magnusdottir G (2014) Forcing of the wintertime atmospheric circulation by the multidecadal fluctuations of the North Atlantic ocean. Environ Res Lett 9(3):034,018+. doi:10.1088/1748-9326/9/3/034018

Rahmstorf S (2002) Ocean circulation and climate during the past 120,000 years. Nature 419(6903):207–214. doi:10.1038/nature01090

Ramankutty N, Evan AT, Monfreda C, Foley JA (2008) Farming the planet: 1. Geographic distribution of global agricultural lands in the year 2000. Glob Biogeochem Cycles 22(1):GB1003+. doi:10.1029/2007gb002952

Scaife AA, Copsey D, Gordon C, Harris C, Hinton T, Keeley S, O'Neill A, Roberts M, Williams K (2011) Improved Atlantic winter blocking in a climate model. Geophys Res Lett 38(23):L23,703+. doi:10.1029/2011gl049573

Scaife AA, Arribas A, Blockley E, Brookshaw A, Clark RT, Dunstone N, Eade R, Fereday D, Folland CK, Gordon M, Hermanson L, Knight JR, Lea DJ, MacLachlan C, Maidens A, Martin M, Peterson AK, Smith D, Vellinga M, Wallace E, Waters J, Williams A (2014) Skillful long-range prediction of European and North American winters. Geophys Res Lett 41(7):2014GL059,637+. doi:10.1002/2014gl059637

Stouffer RJ, Yin J, Gregory JM, Dixon KW, Spelman MJ, Hurlin W, Weaver AJ, Eby M, Flato GM, Hasumi H, Hu A, Jungclaus JH, Kamenkovich IV, Levermann A, Montoya M, Murakami S, Nawrath S, Oka A, Peltier WR, Robitaille DY, Sokolov A, Vettoretti G, Weber SL (2006) Investigating the causes of the response of the thermohaline circulation to past and future climate changes. J Clim 19:1365–1387

Sutton RT, Dong B (2012) Atlantic Ocean influence on a shift in European climate in the 1990s. Nat Geosci 5(11):788–792. doi:10.1038/ngeo1595

Swingedouw D, Rodehacke C, Behrens E, Menary M, Olsen S, Gao Y, Mikolajewicz U, Mignot J, Biastoch A (2013) Decadal fingerprints of freshwater discharge around Greenland in a multi-model ensemble. Clim Dyn 41(3–4):695–720. doi:10.1007/s00382-012-1479-9

Vellinga M, Wood R (2008) Impacts of thermohaline circulation shutdown in the twenty-first century. Clim Change 91(1–2):43–63. doi:10.1007/s10584-006-9146-y

Vellinga M, Wood RA (2002) Global climatic impacts of a collapse of the Atlantic thermohaline circulation. Clim Change 54(3):251–267. doi:10.1023/a:1016168827653

Vellinga M, Wood RA, Gregory JM (2002) Processes governing the recovery of a perturbed thermohaline circulation in HadCM3. J Clim 15(7):764–780. doi:10.1175/1520-0442(2002)015<0764:pgtroa>2.0.co;2

Weaver AJ, Sedláček J, Eby M, Alexander K, Crespin E, Fichefet T, Philippon-Berthier G, Joos F, Kawamiya M, Matsumoto K et al. (2012) Stability of the Atlantic meridional overturning circulation: a model intercomparison. Geophys Res Lett 39(20):L20709. doi:10.1029/2012GL053763

Williams KD, Harris CM, Bodas-Salcedo A, Camp J, Comer RE, Copsey D, Fereday D, Graham T, Hill R, Hinton T, Hyder P, Ineson S, Masato G, Milton SF, Roberts MJ, Rowell DP, Sanchez C, Shelly A, Sinha B, Walters DN, West A, Woollings T, Xavier PK (2015) The Met Office Global Coupled model 2.0 (GC2) configuration. Geosci Model Dev Discuss 8(1):521–565. doi:10.5194/gmdd-8-521-2015

Wiltshire A, Kay G, Gornall J, Betts R (2013) The impact of climate, CO2 and population on regional food and water resources in the 2050s. Sustainability 5(5):2129–2151. doi:10.3390/su5052129

Woollings T, Gregory JM, Pinto JG, Reyers M, Brayshaw DJ (2012a) Response of the North Atlantic storm track to climate change shaped by ocean–atmosphere coupling. Nat Geosci 5(5):313–317. doi:10.1038/ngeo1438

Woollings T, Harvey B, Zahn M, Shaffrey L (2012b) On the role of the ocean in projected atmospheric stability changes in the Atlantic polar low region. Geophys Res Lett 39(24):L24,802-n/a. doi:10.1029/2012gl054016

Woollings T, Franzke C, Hodson DLR, Dong B, Barnes EA, Raible CC, Pinto JG (2014) Contrasting interannual and multidecadal NAO variability. Clim Dyn 1–18. doi:10.1007/s00382-014-2237-y

Zickfeld K, Eby M, Weaver AJ (2008) Carbon-cycle feedbacks of changes in the Atlantic meridional overturning circulation under future atmospheric CO2. Glob Biogeochem Cycles 22(3):GB3024+. doi:10.1029/2007gb003118